Macromolecules
ARTICLE

Macromolecules **2009**, *42*, 9561–9567 **9561**
DOI: 10.1021/ma9009774

Phase-Separated Conetwork Structure Induced by Radical Copolymerization of Poly(dimethylsiloxane)-α,ω-diacrylate and *N*,*N*-Dimethylacrylamide

Katsuhiro Yamamoto,*,† Eri Ito,‡ Shuhei Fukaya,† and Hideaki Takagi†

†*Departement of Materials Science & Engineering, Graduate School of Engineering, Nagoya Institute of Technology, Gokiso-cho, Showa-ku, Nagoya 466-8555, Japan, and* ‡*Material Development Section Central R&D, Menicon Co., Ltd. 1-10 Kouzouji 5-chome, Kasugai 487-0032, Japan*

Received May 7, 2009; Revised Manuscript Received September 28, 2009

ABSTRACT: Phase-separated conetwork structure was induced by a radical copolymerization of telechelic polymer, (polydimethylsiloxane-α,ω-diacrylate (PDMS-DA)), and *N*,*N*-dimethylacrylamide (DMAA). The structure development was investigated by *in situ* SAXS measurement. A mixture of PDMS-DA and DMAA was transparent and homogeneous and gave no peak in SAXS profile. The radical copolymerization of both initiated at 303−363 K was successfully done to form fully transparent objects. Peak was observed in SAXS from the resulting polymer, which can be interpreted in terms of Teubner−Stray model, involving a polymer morphology with given a periodicity. The analysis of time evolution of the SAXS profiles (*in site* measurement) revealed that the phase separation occurred via the spinodal decomposition mechanism. The morphology was fixed by solidification of the sample due to cross-linking and glass transition during reaction-induced phase separation. The final structure was interpreted fairly using Teubner−Stray model. Thus, the final structure of the PDMS-DA/DMAA copolymer sample was found to be a bicontinuous and periodic structure (conetwork) in nanometer scale. The structure was also confirmed by TEM.

Introduction

The study on phase separation induced by polymerization of components in an initially miscible mixture has been widely reported. Polymerization-induced phase separation occurs in multicomponent systems such as polymerizations of monomer/polymer mixtures,[1,2] sol−gel reactions,[3,4] and formation of rubber-modified epoxy resin,[5] polyurethane foam,[6] thermoplastic/thermoset polymer alloy, and polyester elastomer. *In-site* measurement of polymerization-induced phase separation was conducted by some researchers using light scattering,[2,5] synchrotron small-angle X-ray measurement (SAXS),[6] rheological measurement, and FT-IR measurement. Reaction-induced phase separation generally proceeds from an initially homogeneous mixture (solution). In most instances, phase separation occurs via liquid−liquid phase separation except for solid−liquid separation to give regular structures during reaction if phase separation occurs via spinodal decomposition. Such a phase separation is caused by an increase in the molecular weight of the polymer and by the change in the interaction parameters with monomer conversion. These changes in the course of reaction drive the system across thermodynamic phase boundaries and result in a transition from homogeneous to a phase-separated state. It can be considered that the final morphology of the copolymers depends on the kinetic competition between phase separation rates and reaction rates and connectivity between phases. Generally, reaction-induced phase separation through spinodal decomposition develops under successive increase in quench depth, meaning the degree of polymerization continuously increases, for example. Inoue et al. carried out computer simulation of the time-dependent concentration fluctuation using the Cahn−Hilliard nonlinear diffusion equation.[8] The simulation revealed that spinodal decomposition in polymer mixtures under the nonisoquench depth yielded the regular two-phase structure as in the case of the spinodal decomposition under isoquench. The coarsening was suppressed by the increase in quench depth. The final structure was strongly dependent on the quench rate.

Copolymerization of two kinds of vinyl monomers gives copolymer including random, alternative, and blocklike copolymers in accordance with monomer reactivity ratio. Blocklike copolymer can form various microphase-separated structures. Recently, structure development was directly observed by *in situ* small-angle neutron scattering measurement during living polymerizations including anionic,[9,10] atom transfer radical polymerization, stable free-radical polymerization, and radical fragmentation transfer polymerization. Random and alternative copolymers have generally homogeneous structure having one glass transition temperature (no phase separation). When a reactive telechelic polymer or macromonomer having molecular weight of more than a few thousands is copolymerized with monomers whose polymer chain is immiscible with the telechelic polymer or macromonomer, it can be expected that the resulting copolymer shows inhomogeneity, e.g., indicating two glass transition temperatures which means phase separation occurs. Iván et al. reported that cocontinuous structures (conetwork) were generated by copolymerization of a telechelic polymer (hydrophobic polydimethylsiloxane (PDMS) or polyisobutylene) with hydrophiphilic acrylate monomer.[11] SAXS, NMR, DSC, and TEM revealed the structure of the resulting copolymer was composed of cocontinuous two phases, having amphiphilicity in the nanometer range. The copolymer having such a structure and amphiphilicity can be utilized as biomaterial, biocompatible materials, and biosensor.[11−17] These works, however, focused on analysis of generated structure. The cocontinuous and periodic structure is expected to be generated by reaction-induced

*Corresponding author. E-mail: yamamoto.katsuhiro@nitech.ac.jp.

Published on Web 11/17/2009

phase separation via spinodal decomposition. Basically, a reaction rate of radical polymerization is generally high, the chain length of polymer grows rapidly, and its molecular weight is determined within a few seconds later of the initiation. The segregation power (χN) between two polymer components is increasing. Since the polymer products can dissolve in monomer at low monomer conversion, the system is still homogeneous. As the concentration of the resulting polymer products increases, the system can be phase-separated. In such a case, it is anticipated that phase separation induced by radical copolymerization proceeds under successive increase in quench depth.

In this paper, the structure formation of copolymer comprising of PDMS-α,ω-diacrylate (telechelic polymer with M_n of 6500) and *N*,*N*-dimethylacrylamide (DMAA) was investigated by *in situ* SAXS during copolymerization in order to discuss mechanism of the phase separation induced by radical copolymerization. And the final morphology was also analyzed from SAXS profiles using the Teubner−Strey model[18] which has been used in the system of water/oil/surfactant or polymer blend with block copolymer as a compatibilizer. We also confirmed the final structure observed by transmission electron microscopy (TEM).

Experimental Section

Materials. Reactive telechelic polydimethylsiloxane-α,ω-diacrylate (PDMS-DA) was synthesized,[19] which has a molecular weight of 6500 and polydispersity of 1.5 determined by SEC (the columns were calibrated by PS standards). *N*,*N*-Dimethylacrylamide (DMAA) was purchased from KOHJIN Co., Ltd., Japan (98%), and distilled under reduced pressure. 2,2′-Azobis-(2,4-dimethylvaleronitrile) (V-65) as an initiator was purchased from Wako Chemical Co., Ltd., and was used after purification by recrystallization.

Radical Copolymerization. First, PDMS-DA (60 wt %), DMAA (40 wt %), and V-65 (0.1 wt %) were mixed with stirring in a vial. One side of the reaction cell made of stainless steel (thickness of 1 mm and inner diameter of 8 mm) was covered with Kapton film (thickness of 12 μm). The mixture was poured into the reaction cell using a disposal pipet. The upper side of the reaction cell was sealed with Kapton film. Radical copolymerization was conducted on heating−cooling stage (Linkam LK-10002 L, Japan High Tech, Co., Ltd.) whose temperature was controlled within 0.1 K. This apparatus can be used for optical microscopy, X-ray scattering, and spectroscopy. The controlled temperature range is 83−773 K. The sample stage (diameter of 2 cm) has a hole with diameter of 1.6 mm in the center. The maximum cooling and heating rate is ∼120 K/min. The mixture was heated at given polymerization temperature from 300 K at a heating rate of 100 K/min in order to start the radical polymerization. The actual sample temperature was monitored with a thermocouple inserted into the sample and confirmed to be controlled within 0.5 K during a polymerization.

Synchrotron Radiation SAXS. The SAXS measurements with synchrotron radiation were conducted at the beamline BL9C and 15A in Photon Factory (PF) of High Energy Accelerator Research Organization in Tukuba, Japan (KEK), and at the beamline BL45XU in SPring-8. A charge-coupled device (C7300, 1024 × 1024 pixels) with an image intensifier (Hamamatsu Photonics Co., Ltd.) (II-CCD) was used as a detector, and the detector was set at a position of 110 (BL9C) and 230 cm (BL15A) apart from sample position. The wavelength λ of X-rays was 0.150 nm. The sample temperature was controlled using Linkam LK-10002 L. Collagen was used as a standard specimen to calibrate SAXS detector. The scattering intensities were corrected for background scattering and sample absorption. All one-dimensional SAXS profiles were obtained by circularly averaging two-dimensional SAXS patterns. The magnitude of scattering vector (q) is given by $q = (4\pi/\lambda)\sin(\theta/2)$, where λ is the wavelength of the X-ray and θ is the scattering angle.

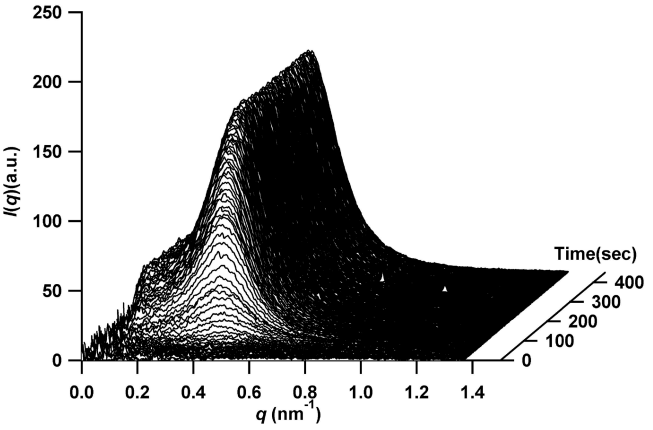

Figure 1. Time dependence of SAXS intensity $I(q,t)$ during copolymerization at 338 K.

Transmission Electron Microscopy. The sample sliced using cryo-ultramicrotome (thickness 80−90 nm) was stained with RuO_4 for 12 h. Transmission electron microscopy images were measured using JEOL JEM2000FX at 200 kV.

Estimation of Conversion. In order to estimate the conversion of monomers, NMR, and DSC measurements were conducted. NMR was performed on a Bruker AVANCE 200 spectrometer using deuterated chloroform at 298 K using protonated chloroform as an internal reference. A small portion of the mixture was extracted and soaked into deuterated chloroform at a given time during polymerization at 338 K. The ^{1}H NMR spectrum of the dissolved parts was obtained. The NMR peaks due to protons on carbons associated with double bond appeared at a range of 5.5−6.8 ppm. The signals at 5.58−5.64 and 5.79−5.84 ppm are assigned to the $=CH_2$ proton in vinyl groups of DMAA and of PDMS-DA, respectively. These signals were used for estimating a monomer conversion because they are observed without overlapping. The peak intensity of these peaks decreases as the reaction proceeds. A differential scanning calorimeter (DSC-22C) manufactured by SEIKO Instruments Inc. was used to measure heat of polymerization. The reaction mixture was heated to the target temperatures at a rate of 65 K/min. The NMR and DSC measurements were measured independently of X-ray scattering.

Results

Synchrotron Radiation Small-Angle X-ray Scattering. Figure 1 shows time dependence of SAXS intensity $I(q,t)$ versus scattering vector q during copolymerization at 338 K. In the early stage of copolymerization, no scattering peak can be observed. The mixture of PDMS-DA and DMAA was homogeneous until the phase separation occurred. The scattering peak at around $q = 0.45$ nm^{-1} first appeared after 70 s, which indicates density fluctuation increase in the reaction system due to phase separation; i.e., this time is regarded as onset of the phase separation. The peak intensity increased until 150 s, after that the peak intensity leveled off. The glass transition temperatures of PDMS and PDMAA were 153 and 373 K, respectively. At copolymerization temperature of 338 K, in the late stage of copolymerization, cross-linking by PDMS chains and vitrification of PDMAA chains occur. Both of them lead to decrease the chain mobility and diffusion. Therefore, at the time after that intensity leveled off, the phase separation was interrupted by cross-linking via PDMS-DA chains and/or vitrification of PDMAA segments. Similar time developments of SAXS feature were observed at the other temperatures.

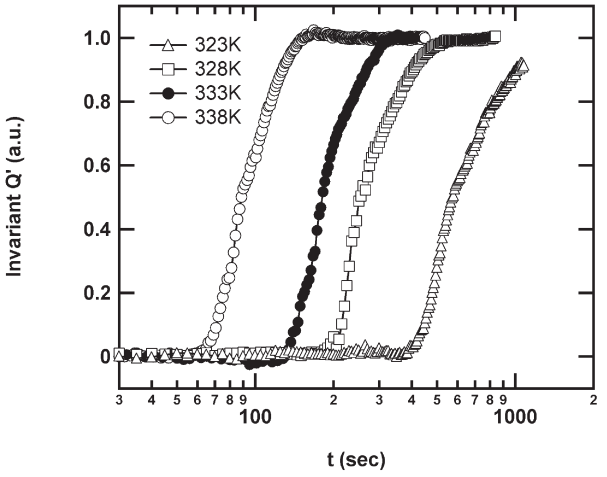

Figure 2. Time evolution of the relative invariant Q' observed at various polymerization temperatures.

The development of scattering intensity (or invariant Q) can be related to the onset of microphase separation during the copolymerization as described above. The invariant is independent of the size or spatial arrangement of the structure inhomogeneities and is expressed as

$$Q = \int_0^\infty I(q)q^2 \mathrm{d}q\phi_1\phi_2(\rho_1 - \rho_2)^2 \qquad (1)$$

where ρ_i and ϕ_i are the electron density and volume fraction, respectively. In this paper, a relative invariant Q' is calculated as integration of $I(q)q^2$ in the range of q between 0.1 and 1.3 nm^{-1}. The relative invariant (the final Q' value was normalized to one) was obtained by in this way. The Q' contributed mainly the real invariant Q, and the change in Q' indicates the development of electron density fluctuation. Figure 2 shows the time evolution of the relative invariant observed at various temperatures. The onset of the phase separation is given as the point where Q' takes off the level in the early stage. The Q' increased rapidly until the phase separation was intercepted, and then it leveled off. The onset time of the phase separation decreased with an increase in polymerization temperature, which is related to formation of PDMAA. Since the generation rate of radicals due to decomposition of the initiator is larger at higher temperature, the formation of PDMAA is much faster. As a result, in the case of high polymerization temperature, the onset time of phase separation induced by the polymerization was short.

Conversion of Monomer with Reaction Time. Monomer conversion and concentration of reactants and products are very important to see the correlation of the conversion with phase separation during the polymerization. Monomer conversion in our system was estimated by NMR and DSC measurements independently of X-ray scattering measurement. The NMR peaks due to protons on carbons associated with double bond in DMAA and PDMS-DA were found to decrease at almost the same rate during the polymerization. DSC measurement during the polymerization allows us to estimate the monomer conversion because the radical polymerization is exothermic reaction. In our case, although all of the double bond in PDMS-DA was not involved in the reaction, the amount of the unreacted double bond in PDMS-DA was negligibly small after the polymerization completed. In addition, the molar ratio of DMAA to PDMS-DA was ~40. Therefore, the observed heat during the polymerization predominantly comes from the polymerization of DMAA. It is possible to correlate the monomer conversions calculated from normalization of the polymerization exotherm in this system. Figure 3 shows heat flow and the obtained and calculated conversions with polymerization time from NMR and DSC measurements, respectively. The onset time of reaction was in the range of 70−110 s. The initiation time was not consistent with the onset time of phase separation revealed by SAXS. The onset time measured by DSC and NMR was always observed slower than the SAXS measurement. During SAXS, the reaction proceeded under X-ray irradiation. In order to see the effect of X-ray irradiation during the polymerization on the onset times, the sample was irradiated with X-rays when only the SAXS data were accumulated for 2 s with time interval of 30 s. This procedure diminished the dose of X-rays. Since it was consequently found that the onset time of phase separation tended to delay without X-ray irradiation, the reason why onset time of the reaction revealed by NMR and DSC measurement dropped back can be ascribed to the enhancement of production of radicals in the system by X-ray irradiation. After the reaction started at 338 K, the monomer conversion rapidly increased and reached over 80% within 100 s. Therefore, the concentration of resulting product sharply grew in a minute after the radical copolymerization was initiated. As shown in Figure 2, the similar trend of development of the invariant Q' was observed. The Q' reached plateau within 80−100 s value after the Q' started to rise. This indicated that the monomer conversion (or concentration of polymer products) strongly linked to the phase separation.

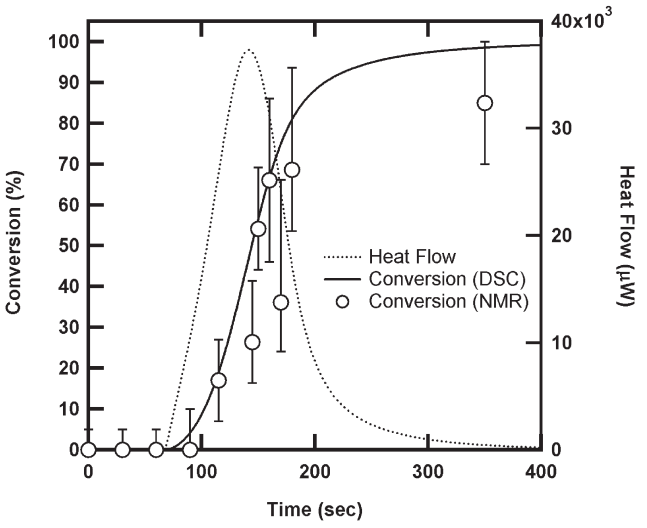

Figure 3. Heat flow and monomer conversions with polymerization time at 338 K.

Discussion

Mechanism of Phase Separation. After a radical copolymerization is initiated, the degree of polymerization increases rapidly and it becomes constant value dependently of reaction conditions (temperature, monomer concentration, initiator concentration, chain transfer constants of chemicals, etc.). Increase in the degree of polymerization N of DMAA gives rise to the segregation power χN between PDMAA and PDMS (χ is Flory−Huggins interaction parameter), and then PDMAA cannot mix with PDMS anymore. However, in a low conversion of monomers, the mixture (resulting polymer, PDMS-DA, and DMAA) is in the homogeneous

state. As the conversion of the monomers increases, the phase separation occurs since the concentration of the polymer rises inevitably. In the case of phase separation of nonreactive binary blend, a quench is usually isothermal, and then the driving force for phase separation remains constant (isoquench). It is easy to think that the quench depth continues to increase as the reaction proceeds in a reactive mixture because the degree of polymerization increases, which is not isoquench conditions. As for a radical polymerization, generally, the length of polymer chain jumped up to be constant quickly, which is governed mostly with the concentration of monomer, initiator, and chain transfer agent. In our case, during the polymerization at constant temperature, the molecular weight of PDMAA might already reach constant value as soon as reaction initiates. Additionally, since the concentration of the resulting products also readily increased, the quench depth was considered to increase continuously as the reaction progressed. The difference in phase separation of our case from nonreactive binary blend, the copolymerization produces additional component such as a kind of block copolymer (poly(DMAA) reacted with one or more PDMS-DA) which acts as surfactants.

Generally, a homogeneous binary (or more) mixture can phase-separate via either nucleation and growth (NG) or spinodal decomposition (SD) mechanisms which are dependent on the quench depth. The NG mechanism leads to a continuous/dispersed phase morphology, whereas the SD mechanism leads to a nonequilibrium bicontinuous morphology in the early stage of phase separation basically. In the case of the NG system which is well characterized, the scattering intensity should decrease monotonically with scattering vector q and grow with square time at a given scattering vector. On the other hand, when phase separation occurs via the SD system, the linearlized theory of Cahn and Hilliard[20] predicts that the compositional fluctuations (the scattered intensity) have a maximum for a given scattering vector. If spinodal decomposition is the mechanism of microphase separation, the peak position q^* in SAXS profile should exponentially increase with time as described in eq 2:

$$I(q,t) = I(q,0)\exp[2R(q)t] \tag{2}$$

where $R(q)$ is the amplification rate of the composition fluctuation[21,22] and depends on q. A plot of ln $I(q)$ versus t should give a straight line during the early stages of phase separation. $R(q)$ is described by

$$R(q) = -D_{\mathrm{eff}}q^2(1+2q^2/{q_{\mathrm{m}}}^2) \tag{3}$$

where D_{eff} is an effective diffusion constant and q_{m} is the magnitude of scattering vector giving maximum $R(q)$.

The strong peak was observed, and the scattering intensity increased with time, while its position shifted to smaller angles at the very early time and then remained constant during the copolymerization. This suggests that the phase separation occurred via spinodal decomposition. At the earliest stage, the SAXS periodicity slightly increased. This fact is not compatible with the expected early stage of the SD under isoquench conditions predicted by Cahn and Hilliard. Practically, the concentration of resulting polymers rapidly increased in this stage; i.e., the amount of monomers, PDMAA, and PDMAA-*co*-PDMS-DA momentarily and continuously changed. When the copolymerization proceeds, it is natural that the specific volume changes and the dilution effect[23,24] on χN emerges since the concentration of

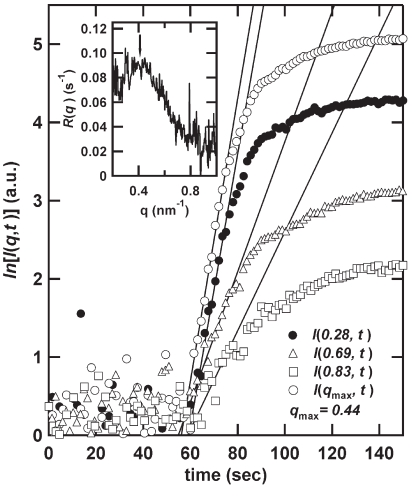

Figure 4. Time evolution of $I(q,t)$ at various scattering vectors. Inset shows exponential growth rates at various q. Polymerization temperature was 338 K.

monomer decreased. It is likely for the periodicity d to change as $d \sim \phi^a$, $\chi \sim \phi^b$ (ϕ is the polymer concentration; a and b are scaling parameters). As generally observed under the conventional thermally induced SD in the intermediate to late stages, it is undeniable that the coarsening process occurred in our system at this time region. Although we could not decide definitively what brought the change of the periodicity at the early time, we analyzed the time-dependent SAXS results using the linearized theory for simplicity.

Figure 4 shows the plot of $I(q,t)$ versus time for some scattering vectors during polymerization at 338 K. Shortly after the beginning of phase separation, a regime where ln$[I(q,t)]$ grows linearly with time was observed. This linear relation allows $R(q)$ to be calculated. A good fit of the ln$[I(q,t)]$ data to a straight line was obtained after the onset of the phase separation at each q. An exponential growth rate, $R(q)$, where the amplitude at q increases are displayed inset in Figure 4. The calculated $R(q)$ was maximum at q_{m} ($q = 0.44$) which is related to the size of the polymer density fluctuation that are the most unstable and which determines the length scale of the initial separated phases. A linear relation between $R(q)/q^2$ and q^2 is expected from the theory of Cahn and Hilliard. The values of $R(q)/q^2$ are plotted against q^2 in Figure 5. The data indicate a linear relation at a low q region, suggesting that the linearized theory can be applied to the early stage of the phase separation even in our case. A deviation from linearity is observed at larger q values. This behavior is attributed to the fact that the linearized theory neglects the random thermal force in isoquench conditions. Most significantly, the deviation is attributed to the radical copolymerization that is occurring during phase separation under successive continuous increase in quench depth.

The effective diffusion coefficient D_{eff} of polymers can be estimated from the extrapolation to $q = 0$ of the linear portion of $R(q)/q^2$.[20]

$$D_{\mathrm{eff}} = \lim_{q \to 0}\left[-\frac{R(q)}{q^2}\right] \tag{4}$$

The magnitude of D_{eff} is a measure in this case. The negative diffusion coefficient indicates diffusion against the concentration gradient (uphill diffusion) as seen in spinodal decomposition of a mixture.[20,26,27] The value of D_{eff} is -1.06 nm^2 s^{-1}. The negative value also strongly supports the SD mechanism in our case.

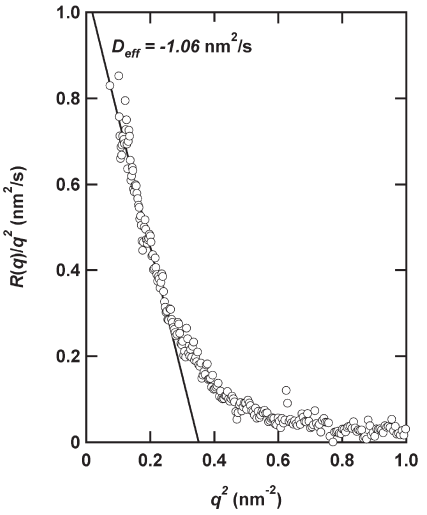

Figure 5. Plot of $R(q)/q^2$ vs q^2 for representation of data obtained for polymerization at 338 K.

Structure Analysis Using the Teubner−Stray Model. In our case, at the onset of microphase separation, the system comprised of PDMAA, PDMS-DA, and block copolymer PDMAA-*b*-PDMS-DA which was formed by polymerization of PDMS-DA with DMAA. Thus, this system is analogy with ternary polymer blend including block copolymer (A, B, A-*b*-B)[25,28−31] and water/oil/surfactant systems[18,32] which showed a microemulsion structure obtained via a spinodal decomposition. In order to study the microemulsion-like structure of our system, the scattering data were analyzed using the Teubner and Strey model.[18] A phenomenological model, based on expansion of a Landau free-energy function, has been developed for bicontinuous microemulsions by Teubner and Strey. Their model describes the scattering intensity in the form

$$I(q) = \frac{1}{a_2 + c_1 q^2 + c_2 q^4} \tag{5}$$

where a_2, c_1, and c_2 are parameters related to a Landau free-energy expansion and q is the magnitude of the scattering vector. This scattering function is equivalent to the real-space density correlation function

$$G(r) = \frac{d}{2\pi r} \sin\left(\frac{2\pi r}{d}\right) \exp\left(-\frac{r}{\xi}\right) \tag{6}$$

and corresponds to a periodic structure modulated by an exponential decay. The characteristic domain size d (periodicity) and the correlation length ξ are related to the scattering parameters via eqs 7 and 8.

$$d = 2\pi \left[\frac{1}{2}\left(\sqrt{\frac{a_2}{c_2}} - \frac{c_1}{2c_2}\right)\right]^{-1/2} \tag{7}$$

$$\xi = \left[\frac{1}{2}\left(\sqrt{\frac{a_2}{c_2}} + \frac{c_1}{2c_2}\right)\right]^{-1/2} \tag{8}$$

Typically, in well-structured microemulsions, c_1 is negative and the model predicts a peak in the scattering spectrum.

The experimental scattering data were fit to eq 5. The data for the sample copolymerized at 338 K are shown in Figure 6.

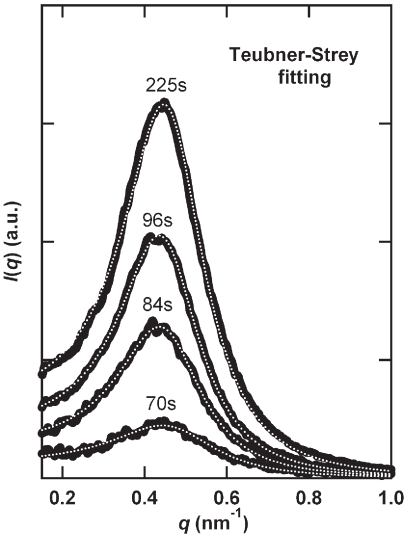

Figure 6. Scattering profiles at selective time of the sample obtained by polymerized at 338 K. The data were fitted by Teubner−Strey model as drawn with dotted lines.

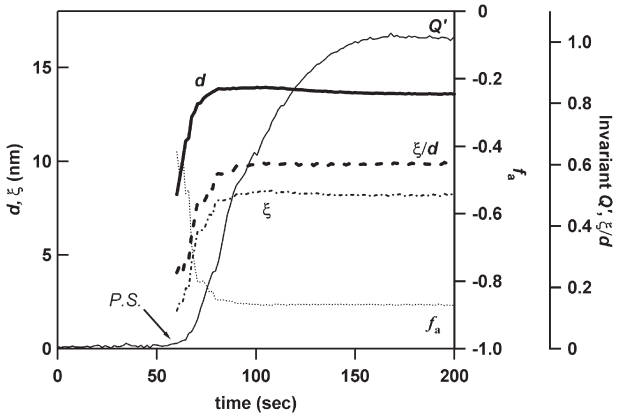

Figure 7. Plot of the characteristic size d (thick line), correlation length ξ (dot-dashed line), and amphiphilicity factor f_a (dotted line) of the sample polymerized at 338 K as a function of time. The d/ξ (broken line) and invariant Q' (thin line) are also plotted as a function of time. Arrow indicates the onset of phase separation (P.S.).

The Teubner−Strey model shows a good fit at each time, indicating the presence of a microemulsion structure in the sample. Figure 7 shows the values of domain size d and correlation length ξ plotted as a function of time. The d showed very slight increase early time, but a short time later it almost leveled off although the invariant still increased. During this period, the concentration fluctuation became large. The value of ξ also increased until the phase separation was constrained by cross-linking and/or vitrification of PDMAA. The ξ/d which is also plotted in Figure 7 increases with time, meaning the increase in concentration of surfactant (in this case block copolymer PDMAA-*b*-PDMS-DA acts as a surfactant) and the decrease in polydispersity of domain size. The block copolymer PDMAA-*b*-PDMS-DA can act as a surfactant to stabilize the mixture of immiscible PDMAA and PDMS. The amphihilicity factor $f_a = c_1/(4a_2c_2)^{1/2}$ has been used to classify the differently structured fluid in the disordered system water/oil/surfactant. This analysis was also used in the ternary polymer blend systems by Morkved et al.[28,29] The time evolution of f_a is also plotted in Figure 7. The value of f_a showed about −0.4 just after phase separation and then decreases to near

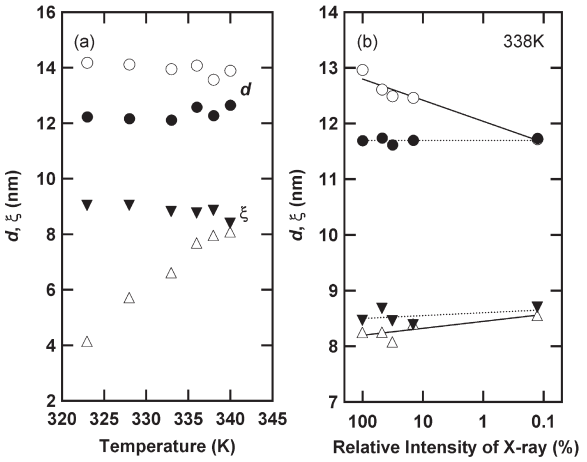

Figure 8. Effect of polymerization temperature (a) and intensity of incident X-rays at 338 K (b) on the characteristic domain size d (circles) and the correlation length ξ (triangles) which were obtained from the scattering on-position (open symbols) and off-position (solid symbols) of X-ray exposure. Lines are drawn for guide to the eyes.

−0.9, indicating the system is near the boundary between a "good" microemulsion ($-1 < f_a < 0$) and a lamellar structure ($f_a < -1$). The structure formed by radical copolymerization of PDMS-DA and DMAA was found to be a bicontinuous microemulsion having a periodicity which was analyzed using Tubner−Strey model.

X-ray Irradiation Effect on the Structure in the Sample. In this paper, *in situ* SAXS experiment was conducted; i.e., the sample was subjected to X-ray irradiation during the structure development. The influence of X-ray irradiation on the structure formation can be imagined. Long exposure time may damage the sample. As the polymerization temperature decreases, the generation rate of radical by decomposition of the initiator is diminished. In this way, the decreasing polymerization temperature requires a long time for a complete of the radical polymerization, resulting in long exposure time for observation of structure development. The structures generated under continuous X-ray exposure during the radical copolymerization were investigated at different polymerization temperatures. In fact, the onset time of the microphase separation increased with a decrease in polymerization temperature, e.g., 130 s at 333 K, 190 s at 328 K, and 390 s at 323 K, as shown in Figure 2. Figure 8a shows the temperature dependence of the characteristic domain size d (circles) and the correlation length ξ (triangles) which were obtained by analysis using Teubner−Strey model. Each scattering data was acquired on-position (open symbols) or off-position (filled symbols) of X-ray exposure after the polymerization completed. The different structural parameters between two cases are clearly seen in the case of lower polymerization temperatures. There is big different in ξ at 323 K. On the other hand, above 335 K, influence of X-ray irradiation on the structure formation was found to diminish considerably because of short exposure time of X-rays, but an unfavorable effect still remained. As a precautionary measure, influence of incident X-ray on the structure of the samples was examined independently from *in situ* SAXS experiment. The X-ray beam was attenuated using an aluminum plate. Scattering data were collected on- and off-positions of X-ray exposure at 338 K. (Here, we made no reference of absolute intensity of X-rays.) The experimental condition at the 100% intensity is the same as that of *in situ* SAXS experiment at 338 K. Each structural parameter was slightly different but within an experimental error. The parameters obtained from the position without exposing of X-rays were independent of incident X-ray intensity. With reduction in intensity of X-rays, the domain spacing obtained from the X-ray exposure position decreased. It was confirmed that the X-ray irradiation eventually had no effect on the structure if X-ray intensity was appropriately controlled. However, the 0.1% of intensity in our experiment is extremely faint so that a time-resolved SAXS measurement cannot be conducted any longer. Although the unfavorable effect remained in the experiment at 338 K, the difference in the structural parameters was considered to be trifling. Thus, the experimental result on 338 K in this study is reliable to discuss the mechanism of structure development.

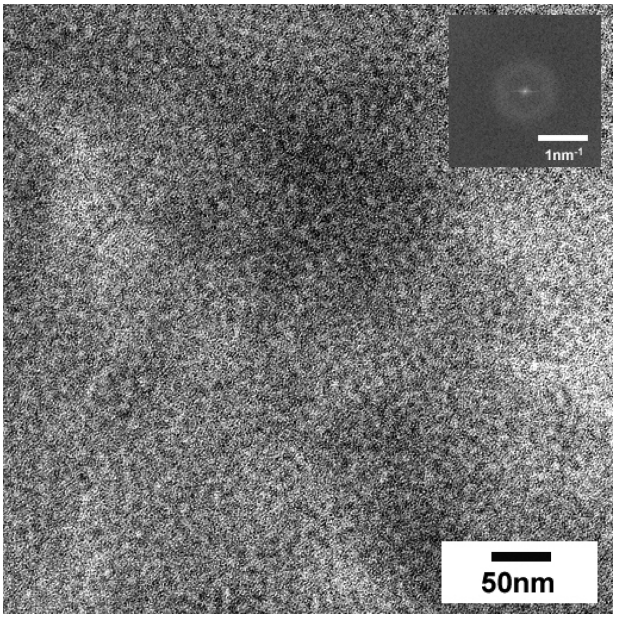

Figure 9. TEM image of the sample polymerized at 333 K. Inset shows 2D-FFT image of the TEM image.

TEM Observation of the Final Morphology. To visually investigate the morphology of the sample, transmission electron microscopy was used. Figure 9 shows the TEM image of the sample polymerized at 333 K which indicates a two-phase bicontinuous structure with no long-range ordering. From analysis of 2D-FFT image (inset in figure), the characteristic periodicity was obtained to be ca.13.3 nm, which is in good agreement with the d obtained from SAXS analysis. The late morphology indicated a periodic and bicontinuous structure, suggesting that cross-linking and vitrification of PDMAA prevent the evolution of a structure with well-segregated domains. As a result, the structure generated at an early stage of spinodal decomposition was preserved.

Conclusion

We investigated copolymerization-induced phase separation using *in situ* SAXS measurement and TEM. It was found that the phase-separated conetwork structure was induced by a radical copolymerization of telechelic polymer, (polydimethylsiloxane-α,ω-diacryalte (PDMS-DA)), and *N*,*N*-dimethylacrylamide (DMAA). The radical copolymerization of both initiated at 303−363 K was successfully done to form fully transparent objects, and they provided peaks in SAXS profiles, indicating the resulting polymers had a periodic structure in nanometer scale. The analysis of time evolution of the SAXS profiles (*in site* measurement) revealed that the phase separation occurred via spinodal decomposition mechanism. The structure was fixed by

solidification of the sample due to cross-linking and/or glass transition during the phase separation. The final structure was interpreted fairly using Teubner−Stray model. Thus, the final structure of the PDMS-DA/DMAA copolymer sample was found to be bicontinuous and periodic structure (conetwork) in nanometer scale. The structure was also confirmed by TEM. The domain size of bicontinuous conetwork structure obtained by SAXS was fairly identical with the value obtained by TEM. The bicontinuous structure consisting of hydrophobic and hydrophilic domains is considered to be desirable as for biomaterials. Hydrophobic (PDMS) and hydrophilic (PDMAA) domains have high permeability to oxygen and ion conductivity, respectively.[33]

Acknowledgment. The SAXS measurement was performed at the Photon Factory of High Energy Accelerator Research Organization (Approval 2008G027) and at SPring-8 (Approval 2009A1177). This research was partially supported by Ministry of Education, Science, Sports, and Culture, Grant-in-Aid for Young Scientists (B) (20750176, 2008). Thanks to Hanaichi UltraStructure Research Institute (Okazaki city, Japan) for TEM observation with great helpful support.

References and Notes

(1) Wang, X.; Okada, M.; Han, C. C. *Macromolecules* **2007**, *40*, 4378–4380.
(2) Okada, M.; Fqjimoto, K.; Nose, T. *Macromolecules* **1995**, *28*, 1795–1800.
(3) Nakanishi, K.; Amatani, T.; Yano, S.; Kodaira, T. *Chem. Mater.* **2008**, *20*, 1108–1115.
(4) Gommes, C.; Blacher, S.; Goderis, B.; Pirard, R.; Heinrichs, B.; Alié, C.; Pirard, J.-P. *J. Phys. Chem. B* **2004**, *108*, 8983–8991.
(5) Ishii, Y.; Ryan, A. J. *Macromolecules* **2000**, *33*, 158–166.
(6) Elwell, M. J.; Ryan, A. J.; Grünbauer, H. J. M.; Van Lieshout, H. C. *Macromolecules* **1996**, *29*, 2960–2968.
(7) Li, W.; Ryan, A. J.; Meier, I. K. *Macromolecules* **2002**, *35*, 5034–5042.
(8) Ohnaga, T.; Chen, W.; Inoue, T. *Polymer* **1994**, *35*, 3774–3781.
(9) Yamauchi, K.; Hasegawa, H.; Hashimoto, T.; Tanaka, H.; Motokawa, R.; Koizumi, S. *Macromolecules* **2006**, *39*, 4531–4539.
(10) Zhao, Y.; Tanaka, H.; Miyamoto, N.; Koizumi, S.; Hashimoto, T. *Macromolecules* **2009**, *42*, 1739–1748.
(11) Domján, A.; Erdödi, G.; Wilhelm, M.; Neidhöfer, M.; Landfester, K.; Ivan, B.; Spiess, H. W. *Macromolecules* **2003**, *36*, 9107–9114.
(12) Iván, B.; Almdal, K.; Mortensen, K.; Johannsen, I.; Kops, J. *Macromolecules* **2001**, *34*, 1579–1585.
(13) Bruns, N.; Scherble, J.; Hartmann, L.; Thomann, R.; Iván, B.; Mühaupt, R.; Tiller, J. C. *Macromolecules* **2005**, *38*, 2431–2438.
(14) Hanko, M.; Bruns, N.; Rentmeister, S.; Tiller, J. C.; Heinze, J. *Anal. Chem.* **2006**, *78*, 6376–6383.
(15) Rimmer, S.; German, M. J.; Maughan, J.; Sun, Y.; Fullwood, N.; Ebdon, J.; MacNeil, S. *Biomaterials* **2005**, *26*, 2219−2230.
(16) Sun, Y.; Collett, J.; Fullwood, N.; MacNeil, S.; Rimmer, S. *Biomaterials* **2007**, *28*, 661–670.
(17) Rimmer, S.; Wilshaw, S.-P.; Pickavance, P.; Ingham, E. *Biomaterials* **2009**, *30*, 2468–2478.
(18) Teubner, M.; Strey, R. *J. Chem. Phys.* **1995**, *87*, 3195–3200.
(19) EU patent EP584826.
(20) Cahn, J. W.; Hilliard, J. E. *J. Chem. Phys.* **1958**, *28*, 258.
(21) Hashmoto, T. *Macromolecules* **1987**, *20*, 465.
(22) Connell, J. G.; Richards, R. W.; Rennie, A. R. *Polymer* **1991**, *32*, 2033.
(23) Sakamoto, N.; Hashimoto, T.; Han, C. D.; Kim, D.; Vaidya, N. *Macromolecules* **1997**, *30*, 5321–5330.
(24) Hanley, K. J.; Lodge, T. P.; Haung, C.-I. *Macromolecules* **2000**, *33*, 5918–5931.
(25) Mallamace, F.; MIcali, N.; Trusso, S. *J. Phys.: Condens. Matter* **1996**, *8*, A81.
(26) Binder, K. In *Materials Science and Technology: A Comprehensive Treatment*; Cahn, R. W., Haasen, P., Kramer, E. J., Eds.; VCH Publishers: Weinheim, 1991; p 405.
(27) Olabisi, O.; Robeson, L. M.; Shaw, M. T. *Polymer-Polymer Miscibility*; Academic Press: New York, 1977.
(28) Morkved, T. L.; Stepanek, P.; Bates, F. S. *J. Chem. Phys.* **2001**, *114*, 7247–7259.
(29) Lee, J. H.; Jeon, H. S.; Balsara, N. P.; Newstein, M. C. *J. Chem. Phys.* **1998**, *99*, 8200.
(30) Jackson, C. L.; Sung, L.; Han, C. C. *Polym. Eng. Sci.* **1997**, *37*, 1.
(31) Hillmyer, M. A.; Maurer, W. W.; Lodge, T. P.; Bates, F. R. *J. Phys. Chem. B* **1999**, *103*, 4814–4824.
(32) Kumura, S.; Seto, H.; Takeda, T.; Nagao, M.; Ito, Y.; Imai, M. *J. Chem. Phys.* **1996**, *105*, 3264–3277.
(33) Nicolson, P. C.; Vogt, J. *Biomaterials* **2001**, *223*, 273–3283.